Crystallographic and Biochemical Analyses of the Metal-Free *Haemophilus influenzae* Fe^{3+}-Binding Protein†

Christopher M. Bruns,‡,§ Damon S. Anderson,|| Kevin G. Vaughan,|| Pamela A. Williams,‡ Andrew J. Nowalk,⊥ Duncan E. McRee,‡ and Timothy A. Mietzner*,||

Department of Molecular Biology MB8, The Scripps Research Institute, 10550 North Torrey Pines Road, La Jolla, California 92037, Department of Molecular Genetics and Biochemistry, University of Pittsburgh School of Medicine, Pittsburgh, Pennsylvania 15261, and Department of Pediatrics, University of Pittsburgh School of Medicine, Pittsburgh, Pennsylvania 15261

Received August 13, 2001; Revised Manuscript Received October 11, 2001

ABSTRACT: The crystal structure of the iron-free (apo) form of the *Haemophilus influenzae* Fe^{3+}-binding protein (hFbp) has been determined to 1.75 Å resolution. Information from this structure complements that derived from the holo structure with respect to the delineation of the process of iron binding and release. A 21° rotation separates the two structural domains when the apo form is compared with the holo conformer, indicating that upon release of iron, the protein undergoes a change in conformation by bending about the central β-sheet hinge. A surprising finding in the apo-hFbp structure was that the ternary binding site anion, observed in the crystals as phosphate, remained bound. In solution, apo-hFbp bound phosphate with an affinity K_d of 2.3×10^{-3} M. The presence of this ternary binding site anion appears to arrange the C-terminal iron-binding residues conducive to complementary binding to Fe^{3+}, while residues in the N-terminal binding domain must undergo induced fit to accommodate the Fe^{3+} ligand. These observations suggest a binding process, the first step of which is the binding of a synergistic anion such as phosphate to the C-terminal domain. Next, iron binds to the preordered half-site on the C-terminal domain. Finally, the presence of iron organizes the N-terminal half-site and closes the interdomain hinge. The use of the synergistic anion and this iron binding process results in an extremely high affinity of the Fe^{3+}-binding proteins for Fe^{3+} (nFbp $K'_{eff} = 2.4 \times 10^{18}$ M^{-1}). This high-affinity ligand binding process is unique among the family of bacterial periplasmic binding proteins and has interesting implications in the mechanism of iron removal from the Fe^{3+}-binding proteins during FbpABC-mediated iron transport across the cytoplasmic membrane.

Processes involving the uptake, transport, and storage of iron are vital to all cellular organisms (*1*). In fact, the requirement for iron is exploited as a form of innate immunity by vertebrate hosts to protect against bacterial infection (*2*). In humans, the host proteins transferrin (Tf) and lactoferrin (Lf) are produced in excess of circulating free iron (*3*) and sequester extracellular free iron at extremely high affinities ($K_d = 1 \times 10^{-21}$ M) (*4*), thereby limiting growth of most microorganisms within this milieu. Disease-causing bacteria, in turn, have developed high-affinity iron uptake mechanisms to compete for this metal with host iron-binding proteins (*5*). If the bacterial pathogen successfully competes for Tf-bound iron, the bacterium is able to multiply and cause disease; if it does not, the bacterial pathogen is generally cleared by the normal host defenses.

Two fundamentally different high-affinity iron-acquisition mechanisms have evolved among bacterial pathogens. The first involves the synthesis of low-molecular weight organic iron chelators that compete for Tf- and Lf-bound iron. This mechanism does not require intimate contact between the bacterial surface and these proteins, and transports iron in the form of an iron chelate (*6*). The second mechanism, in which hFbp participates, is chelate-independent, requires the direct interaction of the host protein and a bacterial surface-associated Tf or Lf receptor, and transports iron into the cell in an unchelated (free) form. This mechanism is summarized in Figure 1 and is well described for pathogenic members of the Neisseriaceae (e.g., *Neisseria gonorrheae* and *Neisseria meningitidis*) and Pasteurelleaceae (e.g., *Haemophilus influenzae*) families. These organisms express Tf and Lf receptors that bind the host iron-binding proteins at micromolar affinities, whereupon iron is extracted directly from Tf or Lf (*7*). This step is typified by binding Tf to the bacterial heterodimeric receptor complex consisting of transferrin-binding proteins A and B (TbpA and TbpB, respectively).

The process by which iron is extracted from Tf and shuttled across the outer membrane and into the periplasmic space remains largely undescribed; however, an energy

† This work was supported by NIH Grant AI33919 to D.E.M. C.M.B. received support from NIH Fellowship F32-AI09937.

* To whom correspondence should be addressed. Telephone: (412) 648-9244. Fax: (412) 624-1401. E-mail: mietzner@pitt.edu.

‡ The Scripps Research Institute.

§ Present address: Incyte Genomics, Palo Alto, CA 94304.

|| Department of Molecular Genetics and Biochemistry, University of Pittsburgh School of Medicine.

⊥ Department of Pediatrics, University of Pittsburgh School of Medicine.

10.1021/bi0156759 CCC: $20.00
Published on Web 11/30/2001

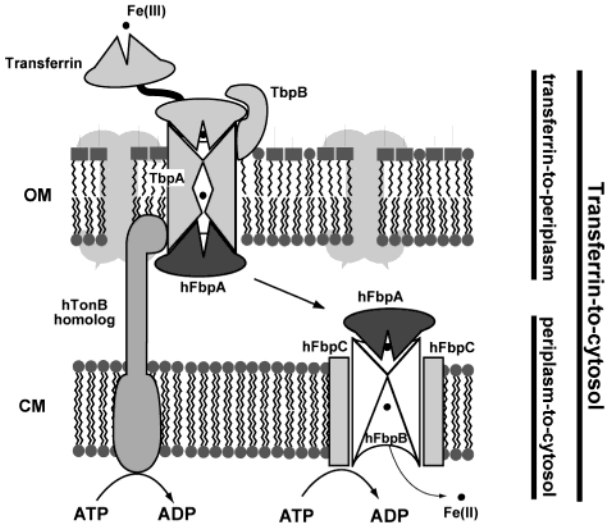

FIGURE 1: Model of free iron transport from transferrin to the cytosol in pathogenic *Neisseria* and *H. influenzae*. Transferrin in the host tissue fluid binds to a specific heterodimeric receptor TbpA/B on the bacterial surface. In this position, free iron is liberated from transferrin, and transported across the outer membrane and into the periplasmic space. Here iron is bound by FbpA and mobilized across the periplasm. Next, the ATP binding cassette (ABC) free iron transporter encoded by the cytoplasmic membrane permease (FbpB) and an ATP binding protein (FbpC) facilitate transport across the cytoplasmic membrane. A key characteristic of this process, which this study addresses, is the reversible binding of iron by FbpA which may be critical for recognition by other components of this iron-uptake system (e.g., FbpB).

source mediated by TonB and associated proteins (ExbB and ExbD) is generally considered to be required (*8*). After transport across the outer membrane, free iron associates with the periplasmic Fe^{3+}-binding protein, designated hFbp (HitA) in *H. influenzae* and nFbp (FbpA) in pathogenic *Neisseria* (i.e., *N. gonorrheae* and *N. meningitidis*) (*9*). Homologues of hFbp and nFbp have been described for other Gram-negative pathogenic bacteria, including *Actinobacillus actinomycetemcomitans* (*10*), *Serratia marcescens* (*11*), *Yersinia enterocolitica*, and others (*10*). Transport of iron from hFbp and homologues across the cytoplasmic membrane is accomplished using a free-iron ABC transporter, consisting of a genetically linked permease and ATP-binding protein (*12*, *13*). Cytoplasmic iron is then assimilated directly into iron-coordinating proteins or prosthetic groups (e.g., heme), or is stored in the form of bacterioferritin (*14*).

Interestingly, while Tf and the Fbps operate in different compartments (serum vs periplasm) and have arisen through separate evolutionary lineages, they are structurally and functionally analogous (*15*, *16*). Similarities between the Fbps and each lobe of the Tfs include an alternating helix−sheet folding motif, the use of a similar subset of amino acid side chains in coordinating Fe^{3+}, the utilization of a synergistic anion as a ternary binding site ligand, and similar Fe^{3+} binding affinities. Extensive biochemical and biophysical analyses, including resolution of the crystal structure of holo-hFbp, have further verified the relatedness of these proteins, leading to the reference of the Fbps as bacterial transferrins (*17*). Both holo-hFbp and holo-half-Tf are composed of two domains, with the iron-binding site occurring in a small cleft between the domains. Recent studies have demonstrated that nFbp indeed has an extremely high affinity for Fe^{3+} ($K'_{eff} = 2.4 \times 10^{18}$ M^{-1}) (*17*), yet as a component of a bacterial ABC-transport system, the binding of Fe^{3+} by Fbp is necessarily reversible. This suggests that Fbp must be able to bind and donate iron and therefore exist as both a metal-bound and a metal-free conformer. In support of this are biochemical studies of the Fbps (*18*) as well as crystal structure analyses (*19*−*21*) and small-angle X-ray scattering experiments (*22*) of other bacterial periplasmic binding proteins that bind non-iron ligands (e.g., sugars and amino acids). These periplasmic binding proteins exist in two structurally different conformations, the transition between which occurs upon ligand binding (*23*, *24*). The unliganded form exists in an open conformation with closure of the two lobes resulting from ligand interaction with the interdomain binding site. The two domains move as rigid bodies about a hinge point located within the central β-sheet connecting them (*25*), termed the "pac man" or "venus flytrap" model (*26*).

Here we report the 1.75 Å resolution crystal structure of apo-hFbp in an open conformation. A surprising finding of this study was that the ternary binding site anion remained bound at the metal ligand site. The measured affinity of apo-hFbp for phosphate in solution was on the order of millimolar. Resolving the structures of both the iron-free and iron-loaded forms of hFbp provides two key snapshots of the iron binding and transport process. Comparison of these structures coupled with an examination of the anion interaction of both of these structures suggests a binding process unique among the family of bacterial periplasmic binding proteins.

MATERIALS AND METHODS

Preparation of Holo- and Apo-hFbp. Recombinant hFbp was prepared by a variation of the previously described method of Adhikari et al. (*12*). Briefly, *Escherichia coli* DH5αMCR containing the plasmid pBSJ1 was grown overnight in 2 L of LB broth containing 100 μg/mL ampicillin. The bacteria were harvested by centrifugation, washed in PBS, and suspended in 50 mL of a 500 mM Tris/2% hexadecyltrimethylammonium bromide mixture (Sigma Chemical Co., St. Louis, MO) followed by shaking at 37 °C for 2 h. The lysate was cleared by centrifugation, and 20 mg of powdered CTAB was added to the supernatant to nucleate overnight precipitation of the detergent at 4 °C. The lysate was centrifuged and separated from the precipitate, then diluted to 400 mL with dH_2O, and centrifuged again. The supernatant was further diluted to 1 L with dH_2O, and run through a CM-Sepharose column connected in series with a DEAE-Sephacel column and equilibrated in 20 mM Tris (pH 8.0). The material passing through both columns was concentrated 15-fold in an Amicon cell using a 10 kDa cutoff Diaflo ultrafiltration membrane and then dialyzed against a 20 mM Tris/200 mM NaCl mixture (pH 8.0), resulting in purified hFbp. For the preparation of all apo-hFbp experiments, trace iron was removed from the buffers using Chelex 100 (Bio-Rad, Richmond, CA) and glassware washed extensively in Chromerge (Fisher Biotech, Pittsburgh, PA) prior to use. hFbp purified as described above was deferrated by adding citrate (sodium salt, pH 7.5) to a final concentration of 10 mM (a 1000-fold molar excess over hFbp), incubating on ice for 30 min, and then dialyzing against 10 volumes of 20 mM Tris (pH 7.5) and 100 mM NaCl at 4 °C, first containing 10 mM citrate, then two times without citrate, and finally twice against 40 mM Tris (pH 7.5) and

Table 1: Apo-hFbp X-ray Data and Refinement Statistics

	8−1.75 Å resolution range	1.86−1.75 Å resolution range
R	0.179	0.37
R_{free}	0.263	0.38
completeness	0.942	0.77
R_{sym}	0.059	0.37
no. of reflections	27754	3703
redundancy	6.7	3.5
rmsd for bond lengths (Å)	0.016	
rmsd for bond angles (deg)	2.22	
rmsd for ΔB (Å^2)	5.0	

100 mM NaCl. All proteins were stored at −80 °C until they were used.

Trypsin Proteolysis of hFbp. Apo-hFbp was dialyzed against 40 mM Tris (pH 7.5) and 100 mM NaCl and digested with trypsin (Sigma) in a solution containing 25 μg of hFbp, 25 μg of trypsin, 40 mM Tris (pH 7.5), 100 mM NaCl, and 25 μM phosphate with or without the addition of 1.2 molar equiv of Fe^{3+} with respect to hFbp. The reaction volume was 125 μL, and the incubation temperature was 25 °C. Aliquots (25 μL) were removed prior to the addition of trypsin and at 5 min, 20 min, 2 h, and 17 h. Digestion was stopped by the addition of an equal volume of 2× SDS sample buffer containing 5% 2-mercaptoethanol and 0.2% SDS and boiling for 5 min. To evaluate the extent of trypsin susceptibility, the samples were separated on a 12% SDS−PAGE gel and visualized by Coomassie blue staining.

UV Difference Spectrophotometry of hFbp. Apo-hFbp was dialyzed against 10 mM MES (pH 6.5) and 100 mM NaCl (spectrophotometry buffer). Protein was then diluted to 0.5 mg/mL (15 μM) with spectrophotometry buffer. Four quartz cuvettes were arranged in a Hitachi model 557 double-beam spectrophotometer (Hitachi Instruments, Tokyo, Japan) such that both sample and reference beams pass through one spectrophotometry buffer cell and one protein cell in tandem. Phosphate was then added to the sample beam protein cell and the reference beam spectrophotometry buffer cell, and an equal volume of spectrophotometry buffer was added to the reference beam protein cell to correct for dilution. Total additions were 2% of the volume of each cell. Spectra were recorded at 25 °C from 300 to 230 nm at 12 nm/min using 1 nm slits. The spectrum at 0 mM phosphate was then subtracted from spectra obtained at variable phosphate concentrations to yield the final spectra. Intensities at 238 nm were plotted against phosphate concentration. Nonlinear regression analysis was performed using Mathematica software.

Crystallization and Data Collection. Apo-hFbp was crystallized by vapor diffusion using the hanging drop method. Crystals belonging to orthorhombic space group $P2_12_12$ (a = 106.7 Å, b = 77.4 Å, and c = 34.2 Å) were grown from a solution containing 28% polyethylene glycol MW 1450 and 100 mM HEPES buffer (pH 6.5). Diffraction data to 1.75 Å resolution were collected from a crystal at room temperature, using a laboratory rotating anode X-ray source and a MAR image plate detector. The data were reduced and scaled using the programs DENZO and SCALEPACK (*27*) and the CCP4 suite of programs (*28*) (Table 1).

Phasing and Refinement. The structure was determined by molecular replacement using the program AmoRe (*29*). The coordinates of iron-hFbp, without metal or phosphate, separated into its two structural domains (*16*), were used as the search model. The model was rebuilt using XtalView (*30*) and refined with TNT (*31*) to the statistics shown in Table 1. The coordinates of *H. influenzae* apo-hFbp are available from Protein Data Bank as entry 1D9V.

Structure Analysis. The separate domains of apo- and iron-hFBP were compared after least-squares superposition using the program LSQKAB in the CCP4 suite of programs (*28*). The position of the hinge axis was deduced from the transformation matrices for the two domains.

RESULTS

Structure of hFbp in the Absence of Fe^{3+}. Comparison of the apo-hFbp structure with that of holo-hFbp reveals a distinct change in the orientation of the two structural domains. Apo-hFbp displays a 21° hinge movement of the two domains relative to the iron-loaded form of the protein (Figure 2). With the release of iron, a cleft is opened in the protein between the two domains, thereby separating the iron binding residues by approximately 5 Å. The residues lining the cleft consist of several charged residues that exhibit extensive hydrogen bonding in the closed state. In the open state, a number of ordered waters are hydrogen bonded between these groups. The number of favorable hydrogen bonding interactions between the two lobes decreases from 19 to just 8 in the transition from the holo- to apo-hFbp form. This movement results in a nominal increase in solvent-accessible surface area of only 496 Å^2, from 13 481 to 13 977 Å^2 [as calculated by DSSP (*32*)], consistent with the limited rotation of Fbp about its hinge in comparison with other binding proteins.

Trypsin Susceptibility Studies. Verification that the open conformer exists in solution was provided by susceptibility to trypsin digestion. This approach has been previously employed to obtain evidence for open and closed conformers of transferrin (*33*) and nFbp (*18*). At limiting trypsin concentrations, apo-hFbp is more sensitive to proteolysis than holo-hFbp (Figure 3), although not to the extent previously shown for nFbp. Nonetheless, this finding demonstrates hFbp adopts the open form in solution and is consistent with apo-hFbp being a less compact structure than the holo form, rendering it more susceptible to trypsin proteolysis.

Iron and Anion Binding Sites. In apo-hFbp, the iron binding residues in the C-terminal domain (Tyr195, Tyr196, and the bound phosphate anion; Figure 4) adopt the same placement and conformation as those in holo-hFbp. In contrast, the binding residues in the N-terminal domain (His9 and Glu57) adopt dramatically altered side chain conformations (Figure 2). Thus, one iron half-site exhibits pre-existing complementarity toward iron, while the other half-site exhibits induced fit. Solution binding experiments, using well-described methods for anion binding by the transferrins, determine a dissociation constant (K_d) for phosphate dissociation from apo-hFbp of 2.3×10^{-3} M (Figure 5). This value is much lower than that of the bacterial phosphate-binding protein, which binds phosphate on the order of 1×10^{-6} M. Despite the structural homology between hFbp and the phosphate-binding protein (*16*), hFbp appears to be a true ferric-binding protein, rather than an iron−phosphate binding protein, since the crystal structure suggests that it is iron that moves in and out while phosphate remains bound in a structural role.

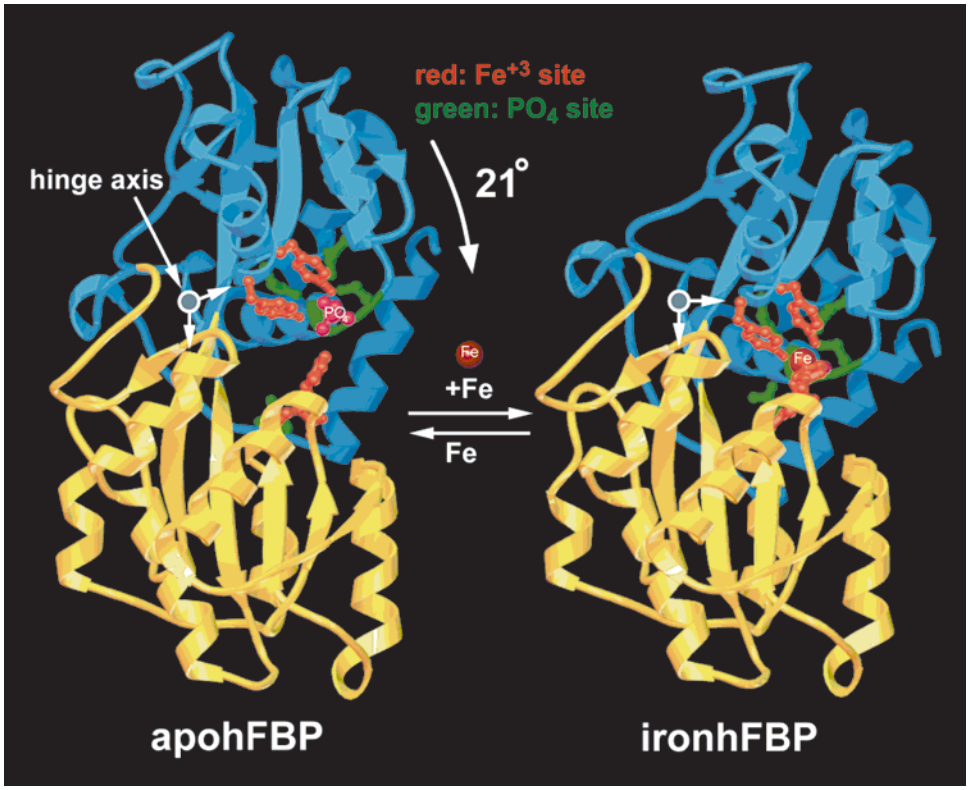

FIGURE 2: Hinge motion upon iron binding in hFbp. The most dramatic difference between apo-hFbp and iron-hFbp is a large relative rotation of the two structural domains. The C-terminal iron half-site (top) retains the same structure in both the apo and iron forms, including the presence of a phosphate ion (pre-existing complementarity), while the N-terminal half-site reorganizes upon iron binding (induced fit).

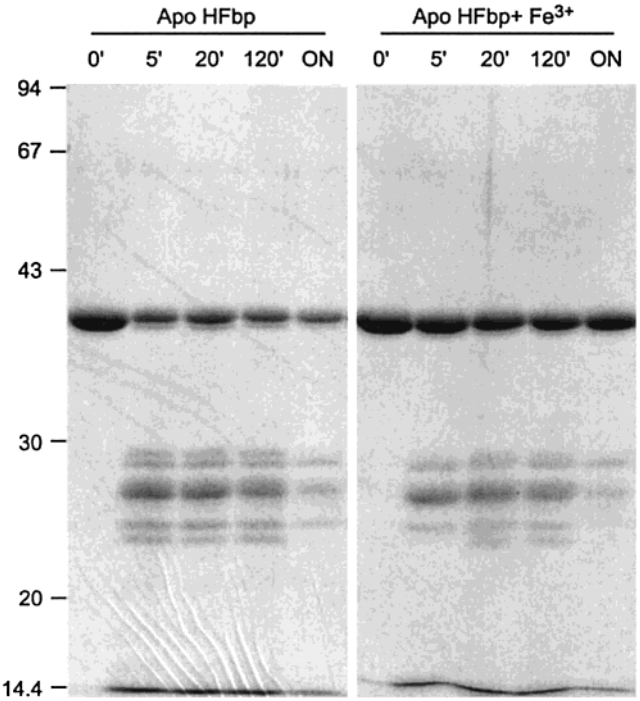

FIGURE 3: Sensitivity of hFbp to trypsin proteolysis. Apo-hFbp is more sensitive to proteolytic degradation than holo-hFbp (compare the first and second panels). In particular, the 5 min time point shows less degraded material in the presence of iron, than it does in the absence of iron. This is consistent with the observed conformational change in the iron-free and iron-loaded hFbp states.

The phosphate ion is less well ordered in apo-hFbp, with a temperature factor of 43 Å^2 versus a value of 18 Å^2 in iron-hFbp (the structures have comparable mean temperature factors of 26.7 and 23.8 Å^2 for main chain protein atoms in the holo and apo forms, respectively). However, the observed contact distances and the presence of an anomalous difference Fourier peak at the anion site of the right size for a phosphorus atom (Figure 4, phosphorus has 0.4 electron of anomalous scattering signal at this wavelength, compared to 0.6 electron for sulfur), along with a measured K_d of 2.3 mM (Figure 5), demonstrate that phosphate ion remains bound in the apo form. The anomalous difference peak on the phosphorus is among the largest in the entire electron density map, and is nearly as large as those of the two sulfurs in the structure. The movement of the N-terminal domain upon the release of iron results in a small displacement of the phosphate toward the C-terminal domain. As a result, the distance between Tyr195 OH and phosphate O4 increases from 2.8 Å in the holo form to 3.3 Å in the apo form. These data are consistent with the premise that, while phosphate is observed in the structure, the anion binding site may be somewhat promiscuous, binding several potential anions diffusing within the bacterial periplasm (see the Discussion).

DISCUSSION

Upon determining the crystal structure of lactoferrin in 1989, Anderson et al. (*36*) noted the folding similarity between each iron binding lobe of Lf and the bacterial periplasmic binding proteins. In addition to the common structural fold, key functional similarities between these evolutionarily disparate families also exist, the foremost being the ability to bind and donate a small ligand. Thus, in a broad sense, the bacterial periplasmic binding proteins and eukaryotic transferrins can be considered a structural and functional superfamily. In this context, hFbp represents a unique position, binding free iron in a manner that is chemically

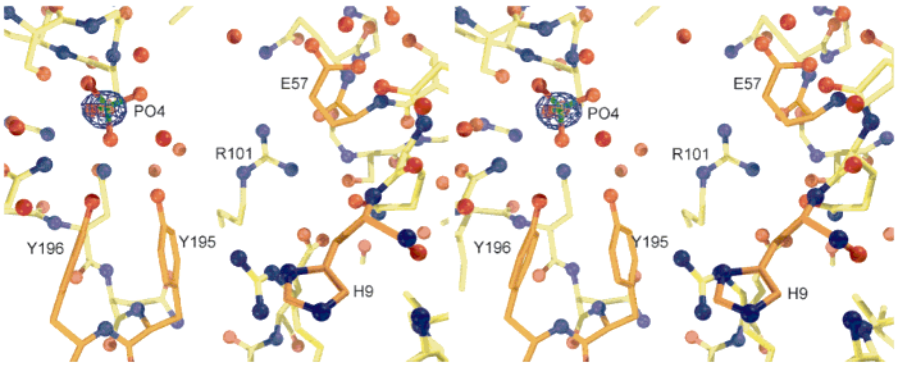

FIGURE 4: Stereopair demonstrating that the anion remains bound in the open conformation of hFbp. Anomalous difference Fourier density at 2.7 Å resolution (contoured at 3σ, blue lines, F^+-F^-, α_{calc}) is consistent with the presence of phosphate at the anion site. The positions of the two tyrosine ligands, Tyr195 and Tyr196, also remain the same, while Glu57 and His9 have swung away from their iron-loaded positions and are now located across the cleft.

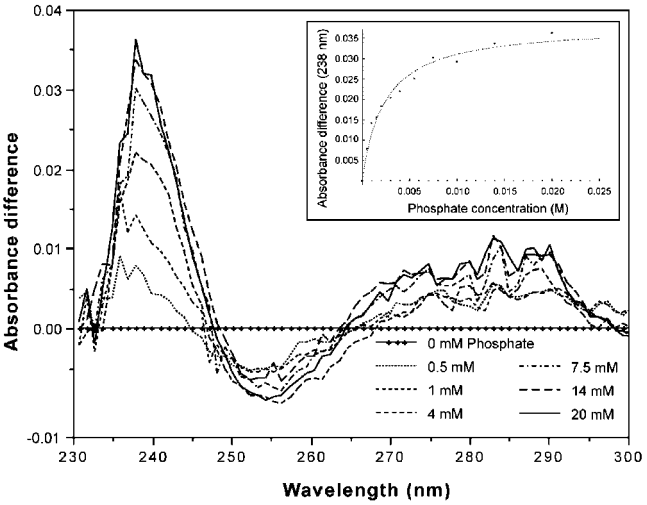

FIGURE 5: Ultraviolet absorbance difference spectroscopic assessment of phosphate binding to iron-free hFbp, using methods previously described for the transferrins. Difference spectra of iron-free hFbp were recorded at various phosphate concentrations. The inset shows the titration curve of iron-free hFbp with phosphate additions, and the absorbance difference measured at 238 nm. Curve fitting to a single-binding site model yields a dissociation constant of 2.3 ± 0.3 mM for phosphate.

analogous to that of the transferrins yet functioning as a bacterial periplasmic binding protein.

In comparing the structure of apo-hFbp to the previously published holo structure, we can be note several structural changes. The most obvious is the 21° rotation of the two structural domains about a central hinge. By comparison, other members of this protein superfamily also exhibit a domain movement upon ligand binding and release, although the motion is usually even larger. A 35° domain swing is observed between the liganded and unliganded forms of maltose-binding protein (Mbp) (*20*); a similar movement of 54° is observed between apo- and holo-Lf (*37*), while in Tf the corresponding motion is 63° (*24*). The general position of the hinge, through two or three β-strands that span the two structural domains, appears to be conserved between hFbp and the superfamily containing the periplasmic binding proteins and the transferrins. As previously reviewed, on the primary and tertiary structural levels, the Fbps more closely resemble the maltose-binding and phosphate-binding proteins than they do the iron−siderophore binding proteins such as FhuD (*38*). Consistent with this, FhuD has an overall structure distinct from that of hFbp (*39*) with a long backbone α-helix connecting distinct N- and C-terminal domains. However, like with hFbp binding to iron, it is predicted that binding of FhuD to the siderophore is unlikely to involve a large-scale opening and closing of the binding site.

The basis for this smaller-scale hinge movement exhibited by hFbp compared with other "typical" bacterial binding proteins may be related to the physical characteristics of the respective ligands. For example, Mbp can accommodate a range of ligands, including both linear and cyclic polysaccharides of varying chain length (*19*). This protein (as well as the majority of other binding proteins) coordinates ligands exclusively through hydrogen bonding interactions, which afford some versatility in the use of specific bonding acceptors and donors. Interestingly, Mbp binds cyclic maltodextrin in the apo conformation, making a large hinge-opening event necessary. Conversely, the Fbps coordinate iron exclusively through ionic bonding interactions, necessitating the use of highly conserved binding residues as well as conserved coordination geometry (*16*). The absolute conservation of the iron binding residues among Fbps from diverse species supports this (personal observation). By comparison to the transferrins, the Fbps undergo a smaller hinge movement most likely due to a much more solvent exposed binding site. Comparisons of the crystal structures of Tf and Lf with hFbp demonstrate that the former binding sites are deeply buried and less solvent accessible due to a surface loop that partially conceals the binding cleft. This difference in binding site accessibility has recently been shown to have other important physicochemical implications, including a profound influence on the $Fe^{3+/2+}$ redox potential for nFbp compared to Tf (*17*).

Although the presence of the ternary binding site anion in the apo-hFbp crystal structure was unexpected, identification of this anion as phosphate presented no surprise as phosphate has been observed within the crystal structure of holo-hFbp as well as identified in other studies (*16*, *17*). Most recently, ^{31}P NMR was employed to identify the presence of phosphate directly and monitor phosphate interaction with Fe^{3+} upon binding by nFbp (*17*). Phosphate associated with the crystals may have come from several potential sources. It may have been a contaminant of the crystallization buffers. Likewise, phosphate-containing apo-hFbp may have selectively crystallized. Supporting this is the observation that hFbp, after being deferrated, becomes fairly unstable at

moderate to high concentrations. Perhaps the presence of phosphate, under crystallization conditions, confers an element of stability to apo-hFbp conducive to crystal nucleation and growth. Regardless, the presence of phosphate in holo-hFbp prepared under similar conditions, the electron density information, and the measured affinity of apo-hFbp for phosphate, in total, support the conclusion that the anion seen in the structure is phosphate.

It is the presence of the ternary anion, and not necessarily its identity, that is the most significant discovery in this structure. In fact, it has become apparent that a number of different oxyanions can fill this role as the ternary ligand, including pyrophospate, arsenate, nitrilotriacetate, citrate, and oxalate, among others (unpublished data). This is consistent with the result that the ternary anion binding site may be somewhat promiscuous, a characteristic perhaps arising from the fact that the Fbps function within the bacterial periplasm where large numbers of diverse anions exist. Versatility in anion binding perhaps contributes physiological flexibility to the process of iron binding and transport across the periplasmic space. Regardless of this promiscuity, it is clear that the presence of the ternary anion plays an essential role in the high-affinity binding process exhibited by the Fbps.

The structures of holo- and apo-hFbp along with biochemical data suggest the following iron-binding process: (1) anion binds to the C-terminal half-site, (2) iron binds to the C-terminal half-site, and (3) the two domains clamp together, completing the iron-binding site. The apo-hFbp structure has a fully formed C-terminal iron-binding half-site, while the N-terminal half-site is disordered. Further, the presence of phosphate in the apo-hFbp structure shows that the addition of exogenous iron, but not phosphate, is required for domain closure. The electrostatic surface of the open form of the protein contains a large negative patch over the phosphate ion with another negative patch on the opposite side of the cleft due to Glu57, one of the iron binding residues (data not shown). In this conformation, the cleft is slightly larger than the radius of the iron atom and an incoming positively charged iron atom would be attracted to this point in the cleft adjacent to the phosphate anion. Part of the reason the phosphate stays bound may be the relatively narrow opening of the cleft, especially when compared to Lf.

The Fbp iron-binding process is unique among the family of periplasmic binding proteins in two main respects. First, although several of the binding proteins can bind a range of related ligands, e.g., Mbp, the lysine/ornithine/arginine-binding proteins, the leucine/isoleucine/valine-binding proteins, D-glucose/D-galactose-binding proteins, etc., none seem to use an exogenous ternary ligand in doing so. In hFbp, the ternary anion contributes one coordination site directly in binding Fe^{3+}. When the ternary anion binds, residues in the C-terminal binding site of hFbp are arranged to create a half-site complementary to binding Fe^{3+}, resulting in the contribution of two additional coordination sites. Thus, the ternary anion serves as an essential factor in contributing exactly half of the Fe^{3+} binding coordination sites. Binding of Fe^{3+} results in nearly optimal octahedral coordination geometry and a high binding affinity (10^{18} M^{-1} for nFbp binding Fe^{3+}), hence the second eccentricity. While this affinity is in a range similar to that of the transferrins, it is 10−12 orders of magnitude higher than that of any of the other periplasmic binding proteins for their respective ligands. Taken together, one could draw the direct correlation between Fbp's unique binding process, which includes the involvement of a synergistic anion, and the extremely high binding affinity which is unique among the periplasmic binding proteins.

The most interesting implication of this binding process is the notion of extremely high-affinity reversible iron binding within the periplasm, in other words, understanding the mechanism by which Fe^{3+} is removed from Fbp upon interaction with the free iron ABC transporter membrane complex. The paradigm of periplasmic binding protein-dependent ABC transporter function, established from systems such as histidine transport ($HisJMQP_2$) (*40*) and others (*41*, *42*), describes a mechanism through which protein interaction of the ABC transporter components coupled with ATP hydrolysis is necessary and sufficient for periplasm-to-cytosol ligand transport. Whether a similar mechanism can be generalized to the FbpABC system, with Fbp exhibiting this extremely high affinity for its ligand, remains to be seen. The mechanism of iron removal from the transferrins involves receptor-mediated endocytosis followed by iron dissociation via vesicle acidification. This low-pH-induced iron dissociation seems unlikely to occur in a localized fashion within the bacterial periplasm. A more probable scheme might involve the action of a periplasmic ferric reductase or a nonspecific reducing agent. Ferric reductases have been shown to exist in the periplasm of a number of bacteria and function in both the maintenance of iron solubility and as a factor involved in ferrous uptake systems (*43*, *44*). Additionally, we have recently reported that nFbp has a positive shift in redox potential compared with Tf; this new potential is on a level compatible with those of physiological reducing groups such as FMN, NADH, and NADPH (*17*). Upon Fe^{3+}/Fe^{2+} reduction, nFbps affinity is estimated to drop to roughly 10^6 M^{-1}, which now approximates the binding affinities exhibited by typical periplasmic binding proteins for their respective ligands. Thus, in addition to a unique binding process, the Fbps may also exhibit a unique process in the removal of iron subsequent to FbpABC-mediated transport.

REFERENCES

1. Welch, S. (1992) in *Transferrin: The iron carrier* (Welch, S., Ed.) pp 1−23, CRC Press, Boca Raton, FL.
2. Weinberg, E. G. (1984) *Physiol. Rev. 64*, 65−102.
3. Welch, S. (1992) in *Transferrin: The iron carrier* (Welch, S., Ed.) pp 25−40, CRC Press, Boca Raton, FL.
4. Welch, S. (1992) in *Transferrin: The iron carrier* (Welch, S., Ed.) pp 68−108, CRC Press, Boca Raton, FL.
5. Neilands, J. B. (1980) in *Iron in Biochemistry and Medicine* (Worwood, A. J. a. M., Ed.) pp 529−572, Academic Press, New York.
6. Neilands, J. B. (1995) *J. Biol. Chem. 270*, 26723−26726.
7. Gray-Owen, S. D., and Schryvers, A. B. (1996) *Trends Microbiol. 4*, 185−191.
8. Cornelissen, C. N., and Sparling, P. F. (1994) *Mol. Microbiol. 14*, 843−850.
9. Mietzner, T. A., Tencza, S. B., Adhikari, P., Vaughan, K. G., and Nowalk, A. J. (1998) *Curr. Top. Microbiol. Immunol. 225*, 113−135.
10. Willemsen, P. T., Vulto, I., Boxem, M., and de Graaff, J. (1997) *J. Bacteriol. 179*, 4949−4952.
11. Angerer, A., Klupp, B., and Braun, V. (1992) *J. Bacteriol. 174*, 1378−1387.

12. Adhikari, P., Kirby, S. D., Nowalk, A. J., Veraldi, K. L., Schryvers, A. B., and Mietzner, T. A. (1995) *J. Biol. Chem. 270*, 25142−25149.
13. Adhikari, P., Berish, S. A., Nowalk, A. J., Veraldi, K. L., Morse, S. A., and Mietzner, T. A. (1996) *J. Bacteriol. 178*, 2145−2149.
14. Andrews, S. C. (1998) *Adv. Microbiol. Physiol. 40*, 281−351.
15. Nowalk, A. J., Tencza, S. B., and Mietzner, T. A. (1994) *Biochemistry 33*, 12769−12775.
16. Bruns, C. M., Nowalk, A. J., Arvai, A. S., McTigue, M. A., Vaughan, K. G., Mietzner, T. A., and McRee, D. E. (1997) *Nat. Struct. Biol. 4*, 919−924.
17. Taboy, C. H., Vaughan, K. G., Mietzner, T. A., Aisen, P., and Crumbliss, A. L. (2001) *J. Biol. Chem. 276*, 2719−2724.
18. Nowalk, A. J., Vaughan, K. G., Day, B. W., Tencza, S. B., and Mietzner, T. A. (1997) *Biochemistry 36*, 13054−13059.
19. Quiocho, F. A., and Ledvina, P. S. (1996) *Mol. Microbiol. 20*, 17−25.
20. Sharff, A. J., Rodseth, L. E., Spurlino, J. C., and Quiocho, F. A. (1992) *Biochemistry 31*, 10657−10663.
21. Hsiao, C. D., Sun, Y. J., Rose, J., and Wang, B. C. (1996) *J. Mol. Biol. 262*, 225−242.
22. Shilton, B. H., Flocco, M. M., Nilsson, M., and Mowbray, S. L. (1996) *J. Mol. Biol. 264*, 350−363.
23. Anderson, B. F., Baker, H. M., Norris, G. E., Rumball, S. V., and Baker, E. N. (1990) *Nature 344*, 784−787.
24. Jeffrey, P. D., Bewley, M. C., MacGillivray, R. T., Mason, A. B., Woodworth, R. C., and Baker, E. N. (1998) *Biochemistry 37*, 13978−13986.
25. Gerstein, M., Anderson, B. F., Norris, G. E., Baker, E. N., Lesk, A. M., and Chothia, C. (1993) *J. Mol. Biol. 234*, 357−372.
26. Mao, B., Pear, M., McCammon, J., and Quiocho, F. (1982) *J. Biol. Chem. 257*, 1131−1133.
27. Otwinowski, Z., and Minor, W. (1997) Processing of X-ray Diffraction Data Collected in Oscillation Mode, in *Methods in Enzymology* (Carter, C. W., Jr., and Sweet, R. M., Eds.) Vol. 276, Macromolecular Crystallography, part A, pp 307−326, Academic Press, San Diego.
28. Collaborative Computational Project No. 4 (1994) *Acta Crystallogr. D50*, 760−763.
29. Navaza, J. (1994) *Acta Crystallogr. A50*, 157−163.
30. McRee, D. E. (1999) *J. Struct. Biol. 125*, 156−165.
31. Tronrud, D. E. (1997) *Methods Enzymol. 277*, 306−319.
32. Kabsch, W., and Sander, C. (1983) *Biopolymers 22*, 2577−2637.
33. Brock, J., Arzabe, F., Lampreave, F., and Pineiro, A. (1976) *Biochim. Biophys. Acta 446*, 214−225.
34. Harris, W., Cafferty, A., Abdollahi, S., and Trankler, K. (1998) *Biochim. Biophys. Acta 1383*, 197−210.
35. Harris, W., Cafferty, A., Trankler, K., Maxell, A., and MacGillivray, R. (1999) *Biochim. Biophys. Acta 1430*, 269−280.
36. Anderson, B. F., Baker, H. M., Norris, G. E., Rice, D. W., and Baker, E. N. (1989) *J. Mol. Biol. 209*, 711−734.
37. Norris, G. E., Anderson, B. F., and Baker, E. N. (1991) *Acta Crystallogr. B47*, 998−1004.
38. Tam, R., and Saier, M. (1993) *Microbiol. Rev. 57*, 320−346.
39. Clarke, T., Ku, S., Dougan, D., Vogel, H., and Tari, L. (2000) *Nat. Struct. Biol. 7*, 287−291.
40. Ames, G. F.-L. (1986) *Annu. Rev. Biochem. 55*, 397−425.
41. Boos, W., and Shuman, H. (1998) *Microbiol. Mol. Biol. Rev. 62*, 204−229.
42. Higgins, C. F. (1992) *Annu. Rev. Cell Biol. 8*, 67−113.
43. Fontecave, M., Eliasson, R., and Reichard, P. (1987) *J. Biol. Chem. 262*, 12325−12331.
44. Worst, D. J., Gerrits, M. M., Vandenbroucke-Grauls, C. M., and Kusters, J. G. (1998) *J. Bacteriol. 180*, 1473−1479.

BI0156759